IOP Publishing | Institute of Physics and Engineering in Medicine Physics in Medicine and Biology

Phys. Med. Biol. **59** (2014) 4583–4602 doi:10.1088/0031-9155/59/16/4583

A comprehensive tool for image-based generation of fetus and pregnant women mesh models for numerical dosimetry studies

S Dahdouh[1,2], N Varsier[2,3], A Serrurier[1,2,4], J-P De la Plata[1,2,5], J Anquez[1,2,6], E D Angelini[1,2], J Wiart[2,3] and I Bloch[1,2]

[1] Institut Mines-Telecom, Telecom ParisTech, CNRS LTCI, Paris, France
[2] Whist Lab, Paris, France
[3] Orange Lab, Issy les Moulineaux, France
[4] Institute of Medical Informatics, Aachen, Germany
[5] InSimo, Strasbourg, France
[6] Theraclion, Malakoff, France

E-mail: dahdouh@telecom-paristech.fr

Received 28 January 2014, revised 29 May 2014
Accepted for publication 16 June 2014
Published 31 July 2014

Abstract

Fetal dosimetry studies require the development of accurate numerical 3D models of the pregnant woman and the fetus. This paper proposes a 3D articulated fetal growth model covering the main phases of pregnancy and a pregnant woman model combining the utero-fetal structures and a deformable non-pregnant woman body envelope. The structures of interest were automatically or semi-automatically (depending on the stage of pregnancy) segmented from a database of images and surface meshes were generated. By interpolating linearly between fetal structures, each one can be generated at any age and in any position. A method is also described to insert the utero-fetal structures in the maternal body. A validation of the fetal models is proposed, comparing a set of biometric measurements to medical reference charts. The usability of the pregnant woman model in dosimetry studies is also investigated, with respect to the influence of the abdominal fat layer.

Keywords: image-based fetal models, articulated growth model, numerical dosimetry

(Some figures may appear in colour only in the online journal)

1. Introduction

The possible deleterious effects of ionizing and non-ionizing electromagnetic radiations on the health of the developing fetus, adults and children have been the focus of several studies (Bibin *et al* 2009, Hadjem *et al* 2010, ICRP 2003, Maynard *et al* 2011, Wiart *et al* 2011). Radiation transport or electromagnetic field (EMF) simulations on realistic numerical models of the pregnant woman body and the developing fetus are used to compute the correlation between health effects, fetal absorbed dose and age (Maynard *et al* 2011).

Three different coding approaches can be distinguished (Bibin *et al* 2009) to generate the numerical models: purely mathematical models, voxelized models and synthetic ones.

Easy to implement, the mathematical models describe the anatomical structures using surface equations as in Cristy and Eckerman (1987). In Stabin *et al* (1995), the authors developed a simplified version of the human fetus, later refined by Chen *et al* (2004) leading to three pregnant women models at 3, 6 and 9 months of gestation.

Despite their usefulness and the easiness of their implementation, the lack of anatomical realism of these models is considered as a major drawback, in particular within the radiofrequence band, and they tend to be less and less used. To overcome these issues, other modeling approaches such as the two presented next have been developed.

Voxelized models are built from segmented medical images. In Shi and Xu (2004), a 30 week old fetus was constructed based on the segmentation of a CT volume aquired on a pregnant woman. However, because of the limited spatial resolution, fetus details were not included in the model. Moreover, the limited field of view of the scan did not encompass fully the fetal head. The maternal trunk was modeled in Angel *et al* (2008) from segmented CT images between the 12th and 36th weeks of gestation, distinguishing soft tissues from bones, and modeling the uterus and the gestational sac. Using a study performed on 24 patients, voxelized female abdominal models were created. Fetal models were composed of fetal bones and soft tissues without distinguishing between them.

Although being the preferred method by many authors due to the realism of the anatomical structures, such models are hard to obtain due to lack of 3D medical images with a large field of view and the amount of work needed to manually segment these data. Indeed, in the case of pregnant woman, whole body images are difficult to acquire for ethical (related to the non-essential fetal exposure) as well as technical limitations (related to long scanning time and limited field of view). Thus, while useful, the use of such models remains limited since the whole woman body is not modeled, and thus pregnant woman and fetus exposure to waves cannot be measured accurately.

A third generation of anatomic computational models consists of hybrid phantoms combining computer graphics methods and voxelized models (de la Plata Alcalde *et al* 2010). In Dimbylow (2006), four mathematical models representing the utero-fetal unit (UFU) were voxelized and inserted into a non-pregnant woman. This insertion required several voxel editing steps. In Xu *et al* (2007), hybrid models combining the UFU and maternal organs previously published in Shi and Xu (2004), the VIP-MAN model from Xu *et al* (2000) and a synthetic model of the fetus surface were used to construct the 3D surface model of a pregnant woman (at 3, 6 and 9 months of pregnancy). The heterogeneous woman model was composed of several organs and fetal soft tissues, brain and skeleton could be distinguished in the fetal model. The UFU insertion was performed through manual deformations. In Nagaoka *et al* (2008), a voxelized model of the UFU at 26 weeks of gestation was built based on the segmentation of magnetic resonance imaging (MRI) data. This model was used to generate two other ones at 13 and 18 weeks of gestation, by downscaling. The three models were finally inserted inside a heterogeneous non-pregnant woman. In Becker *et al* (2008), a 24 weeks of

pregnancy old virtual pregnant woman, named Katja, was constructed from two voxel models, one from an abdominal MRI segmentation of a pregnant patient and the second one from the segmentation of a non-pregnant woman. The UFU insertion was performed using a dedicated software specialized in voxel editing. In Bibin *et al* (2010), a hybrid pregnant woman model covering different stages of pregnancy (from 8 to 12 weeks of amenorrhea (WA) and from 26 to 34 WA) was constructed. Different approaches were developed depending on the type of data used. During the first trimester, data consisted of 3D US images and a semi-automatic approach for separating amniotic fluid from maternal and fetal tissues was used, while during the last trimester MRI data allow more detailed fetal modeling. In Maynard *et al* (2011), two fetal hybrid computational phantoms were constructed using high-quality MRI and computed tomography images from two fetal specimens at 11.5 and 21 weeks of gestation. After manual segmentation and upload into a 3D modeling software, the two aforementioned specimen phantoms along with a modified version of a 38 week newborn one was used to construct 8 heterogeneous computational models from 8 to 38 weeks of gestation.

While representing significant advance over other available models in terms of fetal ages and processing of main major soft tissue organs and the developing skeleton, the previous method does not cover the embryonic stage and not all the fetal ages are represented. Using this method, studying the fetal positioning influence on dose computation is also not possible.

In order to overcome these issues, the work presented in this paper focuses on the construction of a pregnant woman model from 8 to 32 weeks of amenorrhea (WA) covering most of the embryonic and fetal ages. Two different approaches are developed depending on the stage of pregnancy. For the fetal phase, body repositioning is made possible for fetal limbs and head, allowing the investigation of fetal pose influence on dose exposure. The model is also easily extendable to encompass more fetal soft tissues.

While other papers rely heavily on manual segmentation, the aim of this work is to develop semi-automatic tools in order to be able to easily enrich the models and create new ones. Once created, the fetus (for the rest of the study, except specifically specified, fetus will denote both embryo and fetus) is inserted into a simplified ellipsoidal uterus composed of the uterus wall and the amniotic liquid. The whole Utero Fetal Unit (UFU) will then be automatically inserted in a semi-homogeneous non pregnant woman model using the method presented in de la Plata Alcalde *et al* (2010). Once done, this model will be used to assess the fetal exposure to plane waves throughout all stages of pregnancy. The main contribution of this paper is to gather segmentation, 3D modeling, deformation, interpolation and simulation methods to build a complete processing chain, from image data to the generation of realistic models at any age and in any position, to be used to obtain dosimetry simulation results.

The first part of this paper thus focuses on the construction on the fetal growth modeling tool. First, the data used are presented. Then, the two different algorithms developed for embryo and fetal modeling are described. The construction of the corresponding UFU is then explained and finally its insertion in a non pregnant woman concludes the modeling part of this paper. The remainder focuses on an analysis of the exposure of the pregnant woman and the developing fetus to radiofrequency electromagnetic fields.

2. Medical data

3D US data of entire fetuses are easily available during the first trimester of pregnancy but nearly never accessible during the second and third trimesters, the fetus being often too big to fit in the US probe field of view, and the US inherent noise making the data really difficult to process.

Figure 1. Slices of three 3D US volumes at different stages of gestation (WA: weeks of amenorrhea).

Thus, several sets of medical images of various modalities representing different fetuses were used for this project. They cover the gestation period from 8 to 34 WA and will serve as references from which any age and position will be modeled.

Embryonic data. Eighteen volumes of ultrasound (US) images of embryos and fetuses from the first trimester of pregnancy (from 8 to 13 weeks of amenorrhea) were provided by the Beaujon AP-HP hospital (France). Examples of 3D US slices can be seen in figure 1. They were acquired using a Voluson 730 Expert system (GE) with a 3.7–9.3 MHz transvaginal volumetric probe and present isotropic voxels with a spatial resolution ranging from 0.21 to 0.96 mm^3.

Fetal specimens. Fetal specimens were obtained from a series of well-preserved fetuses from the Anatomy Laboratory in Montpellier. The collection, preserved in formalin for several decades, is composed of 20 fetuses with unknown exact age (up to 20 WA) and origin. Two specimens were imaged using micro Computer Tomography (μCT) with a resolution of 3.6 μm. The ages (14 and 16 WA) of the specimens were estimated by cross-correlation of different measurements such as crown-rump length, head circumference and femur length, and compared to fetal measurement charts (Guihard-Costa and Larroche 1995). The quality of the CT images was highly variable, with a really low contrast and a little ossification possibly due to the formalin conservation method. Figure 2 shows one fetus as well as one slice of the corresponding μCT volume.

Fetal data. Twenty two MRI volumes, acquired with Steady State Free Precession (SSFP) sequences (Anquez *et al* 2007), between 26 and 34 WA, were gathered at Saint Vincent de Paul hospital (Paris, France). Two CT volumes of the full trunk of pregnant women at 27 and 32 WA were collected at the Kremlin Bicetre hospital. These CT-scans were part of a clinial protocol and were performed to assess the evolution of maternal pathologies. Those pathologies did not hinder the quality of data and fetal skeletons were normal.

Table 1 summarizes the different sets of data selected to construct the embryo and fetal models presented in this study.

Using complementary 3D imaging modalities allows us to cover a large range of gestational ages and visible structures. All the images were recorded on pregnant women during medical examinations except the two sets of μCT. Each modality is exploited according to the structures of interest that are visible on the corresponding images.

Since all the structures are not visible on all data, different strategies were designed to construct embryonic and fetal models as explained next. A 3D mesh model of a 20 WA from the National Institute of Information and Technology of Tokyo was also used.

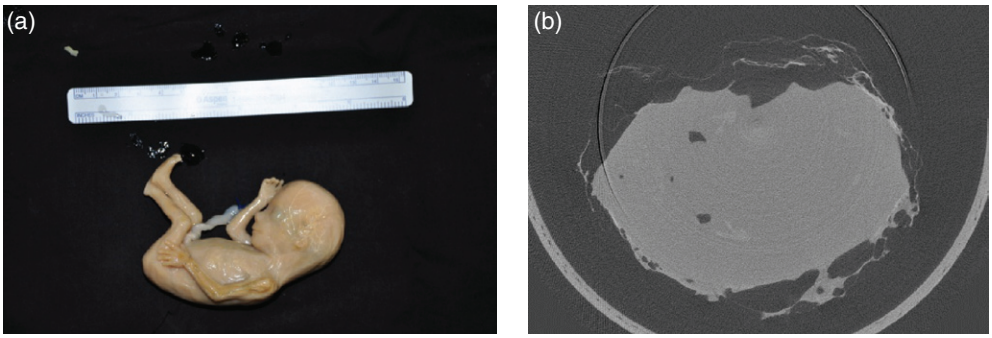

Figure 2. Fetus at 14 WA and a slice of the corresponding μCT volume.

Table 1. Image Database.

Modality	Pregnancy Stage (WA)	Slice thickness (mm)	Image resolution (mm/px)	Subject	Structures of interest
CT	27	1.2	0.64	*In vivo*	skeleton
CT	32	1	0.96	*In vivo*	skeleton + envelope
μCT	14	0.048	0.036	Formalin	skeleton + lungs + brain
μCT	16	0.144	0.036	Formalin	skeleton
MRI	20	0.74	0.74	*In vivo*	brain
MRI	26	1.6	1.36	*In vivo*	brain + lungs
MRI	30	4	0.94	*In vivo*	brain + lungs
MRI	32	4	0.94	*In vivo*	brain + lungs
MRI	34.5	4	0.94	*In vivo*	brain + lungs
3D US	8	2.4	2.4	*In vivo*	brain + envelopeuterus + placenta + amniotic liquid
3D US	9	2.3	2.3	*In vivo*	brain + envelope + uterus + placenta + amniotic liquid
3D US	10	7.9	7.9	*In vivo*	brain + envelope + uterus + placenta + amniotic liquid
3D US	12	5.6	75.6	*In vivo*	brain + envelope + uterus + placenta + amniotic liquid
3D US	13	7.6	7.6	*In vivo*	brain + lungs + envelope + uterus + placenta + amniotic liquid

3. Fetal growth modeling

3.1. Embryo modeling

In order to model embryos during the first trimester of pregnancy, a segmentation method for extracting the fetus envelope on 3D obstetric ultrasound images has been developed in Dahdouh *et al* (2013). This method integrates a shape constraint into a 3D multi-phase variational segmentation approach, extending the two-phase framework introduced in Anquez *et al* (2013) where authors embedded a pixel intensity distribution prior into a two phase level-set framework in order to separate fetal and maternal tissues from the amniotic fluid. The framework used to construct the embryo models is a shape-guided variational segmentation method combining three different types of information: pixel intensity distribution, shape prior on the fetal

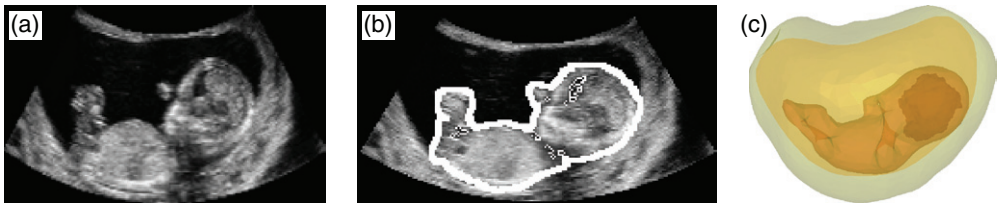

Figure 3. (*a*) Slice of a 3D US volume. (*b*) Segmentation of the fetal envelope using the framework proposed in Dahdouh *et al* (2013). (*c*) Utero Fetal Unit reconstruction with amniotic fluid (green), the placenta (yellow), the fetal envelope (orange) and the brain (brown).

envelope and a back model varying with the fetus age. More precisely, an energy functional is defined over the image measuring the quality of an initial partition of the voxels into different tissue classes. It is then optimized using the level-sets formalism (Vese and Chan 2002). Tissue intensity distributions, shape priors encoded with legendre moments, and contour length measures compose the energy functional. A set of shape models is learned to encode the variability of the fetus shape and position. Combination of these terms into a four-phase level-set framework allows us to handle the lack of contrast and explicit boundaries in US images. A back model is used in a post-processing step to separate the fetus from connected structures.

Finally, the brain is manually segmented and added to the resulting segmentation, as well as the placenta, the amniotic fluid and the umbilical cord.

An example of a resulting embryo model is shown in figure 3.

During the first few months of pregnancy, limbs and body parts are not easily separable. Thus, we decided here not to focus on the creation of an articulated model, and positioning is handled solely through a set of simple geometrical transformations such as rotations of the whole body. The only exception could be for the 13 WA fetus were limbs are more easily identifiable. However, since the skeleton is hard to visualize and obtain on 3D US images, we decided not to develop a deformation method specifically for this age and the 13 WA was handled the same way we handled the other embryos.

Both manual and automatic segmentation results have been validated quantitatively and visually by a medical expert (Dahdouh *et al* 2013).

3.2. Fetal modeling

While 3D MRI data can easily be gathered during the third trimester of pregnancy, they are really difficult to obtain during the second one due to larger fetus movements during this period. The lack of appropriate data during the second trimester of pregnancy led us to develop a different strategy for fetal modeling.

3.2.1. Image segmentation. For MRI data, brain and lungs were segmented using the method presented in Anquez *et al* (2009). First, using an automatic detection and segmentation of the eye balls, an average brain shape model is registered and refined to segment the brain. Second, a set of automatically detected landmarks, combined with manual ones, is used to determine the fetus orientation. Third, an articulated skeleton model is registered using these landmarks. This registration provides an initialization to a graph-cut procedure used to segment the fetal envelope. Lungs segmentation is performed using the previously determined landmarks.

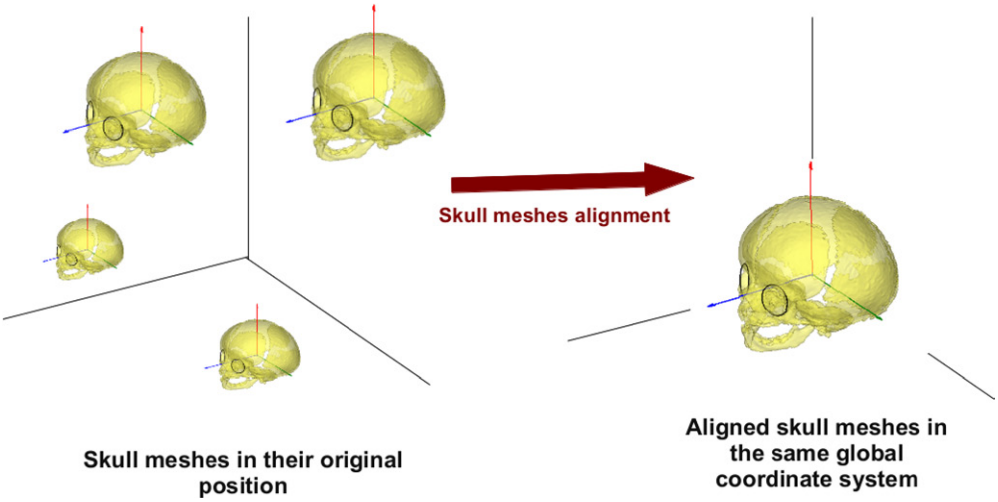

Figure 4. Skull mesh alignment using orbits and the center of mass of the head as landmarks.

Semi-automatic segmentation procedures were used for the skeleton and the fetal envelope on CT-scan and μ-CT data after a pre-processing aiming at enhancing the contrast and reducing the high frequency noise. Surface triangular meshes were generated for each structure.

3.2.2. Skeleton and soft tissues modeling. Instead of constructing different models from the segmentation of medical images, a growth modeling tool throughout the second and third trimesters of pregnancy is developed as explained in Serrurier *et al* (2013).

In order to be able to perform an interpolation between the meshes of equivalent structures in the database, a topology unification procedure is applied. First, for each structure, a mesh is chosen as reference and then deformed towards the other meshes at each age using a set of manually and automatically selected landmarks and a 3D Moving Least Square procedure (Zhu and Gortler 2007). The meshes derived from the CT data at 32 WA for the skeleton, being more precise and of higher quality, are chosen. For the brain and lungs, the meshes derived from the MRI images at 34.5 WA, being the more detailed, are used. This topology unification procedure generates, for each structure and at all the considered ages, meshes with identical topologies which is critical to be able to study and simulate body parts evolution. The deformed meshes are used, instead of the original ones, for the rest of the study.

To simulate body parts evolution with regard to time, meshes need to be registered. A local coordinate system is thus defined for each of the skeleton parts and each organ, based on anatomic and geometric considerations. The local frames are then aligned to a common global coordinate system as shown in figure 4. The transformations include rotation and translation and are optimized using correspondence between landmark points.

This operation was done independently for each individual structure.

After alignment, a linear interpolation is performed between ages so that structures shapes can be estimated at any age. Meshes of the different skeleton sections are then assembled together to form a fetus in the desired position. Articulations between the skeleton sections are derived from the observed articulations of the fetuses of the database using geometrical considerations. Using landmarks determined on nearby bone structures, articulations

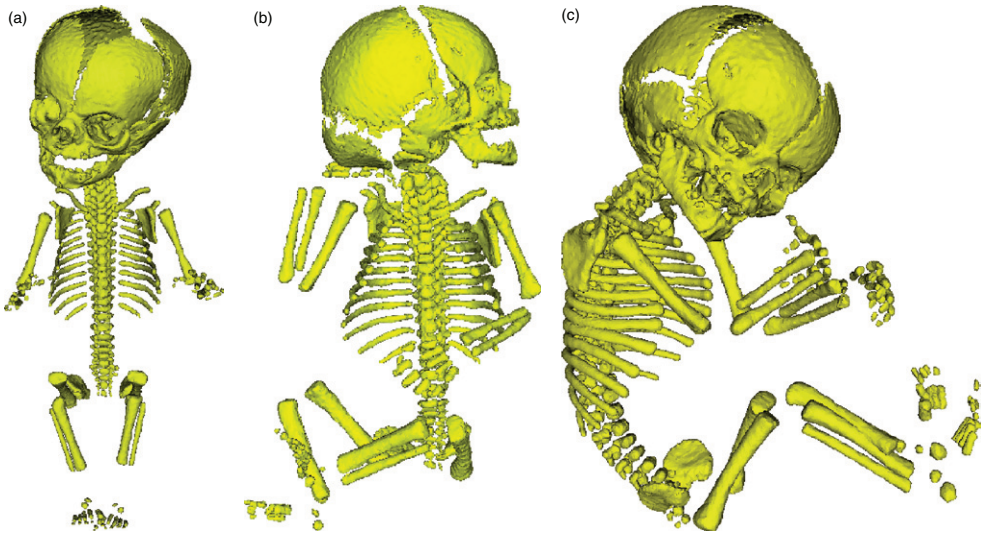

Figure 5. Generic fetal skeletons at different ages and positions using the proposed method.

are constructed in relation to the relative position of structures of our database. Finally, the meshes of the internal organs are positioned in relation to their underlying skeleton structures, using landmarks and mean relative positioning of each landmark determined on our database.

3.2.3. Fetus repositioning. Since the skeleton is reconstructed using artificial articulations, fetal positioning can be modified easily within a set of anatomically realistic positions by controling the articulation angles. Figure 5 illustrates the ability of the method to generate fetuses at multiple ages and positions.

Regarding spine articulation, we decided not to include any articulation in it. For a same global position at different ages, the fetus is less curled up at the early stages than at the late stages of pregnancy. This reflects the fact that along the fetal growth, the space available for fetal movements becomes more and more limited and thus fetuses tend to adopt a more curled up position. Our model will thus tend to be more and more curled up at later ages.

3.2.4. Body envelope reconstruction. A different strategy had to be developed for the body envelope. Indeed, its shape varies according to the age of the fetus but also, unlike the other structures, according to the position of the fetus, regardless of its age. A strategy based on linear interpolation of envelopes aligned in a local coordinate system appears thus heavy and inappropriate, implying a pre- and post-deformation of the envelope mesh to go through a neutral position for the interpolation. We decided rather to use a skeleton driven deformation method. A single generic envelope mesh (the one corresponding to the 32 WA fetus) is deformed towards the desired fetus according to its skeleton.

First, the generic envelope mesh is decomposed into several sub-components according to the underlying skeleton sections as shown in figure 6. Each subpart is then deformed, using a Moving Least Square deformation procedure, according to the deformation of the underlying skeleton section. This result in a fetal envelope with non-smooth transitions between subparts as shown in figure 6.

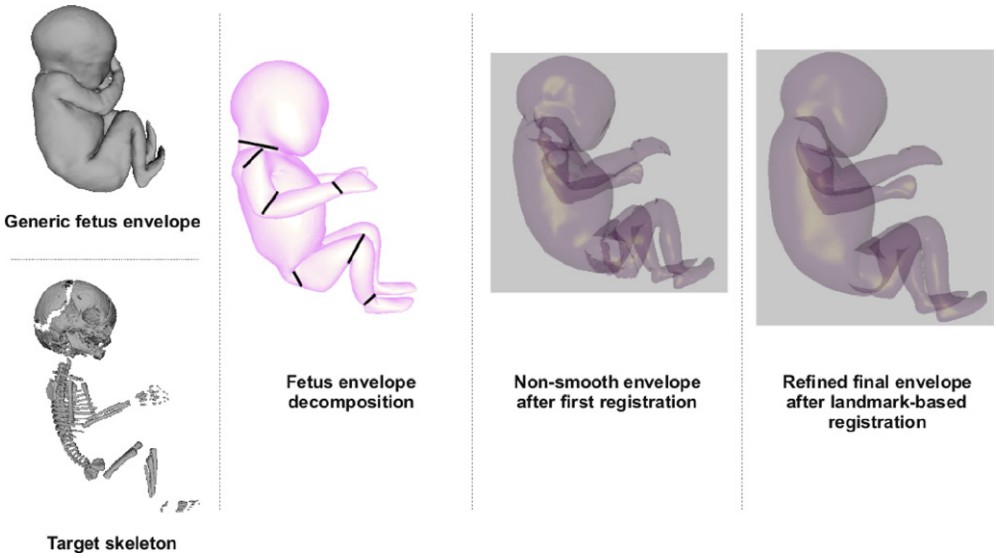

Figure 6. Mapping of a generic fetal envelope on a target skeleton, via envelope decomposition, according to skeleton sections and MLS deformation.

Since the initial and deformed envelopes have the same topology, a global MLS deformation between the inital envelope and the one resulting from the local deformations is performed to overcome this issue. A set of landmarks is randomly selected on all the deformed sub-envelopes and their equivalents on the initial envelope are computed. A global deformation to align the two sets of landmarks using a MLS procedure with a geodesic distance is then performed to obtain a final envelope with smooth articulations as shown in figure 6.

Using the method described above, by linearly interpolating between the subjects of the database, each structure can be estimated at any age and in any position. This process results in an automated modeling tool, the operator being only required to specify the age and position of the desired fetus. Available ages are from 14 to 32 WA, the model being limited by the skeleton information unavailable before and after these ages. The models are all composed of the fetal envelope, the skeleton, the brain and the lungs. More details about fetal model construction and positioning can be found in Serrurier *et al* (2013).

3.2.5. Growth modeling tool interface. Since one of the aims of this study is to propose a simple tool for generating fetus models, the method proposed above has been automated and implemented into a user-friendly software. The user is first asked to enter various angle parameters defining limbs and head positions and the desired fetus age. Twenty parameters defining 28 different deformations around several articulations such as elbows, knees angles, or head orientation can be configured. Once the fetus is positioned, the fetal skeleton as well as internal organs and envelope can be generated. This can be done at the initial chosen age used to configure positioning or the user could choose to use the skeleton position previously parameterized to generate fetuses at different ages with the same position. After the fetus generation, the user can choose to generate the surrounding uterus and amniotic liquid, as described next.

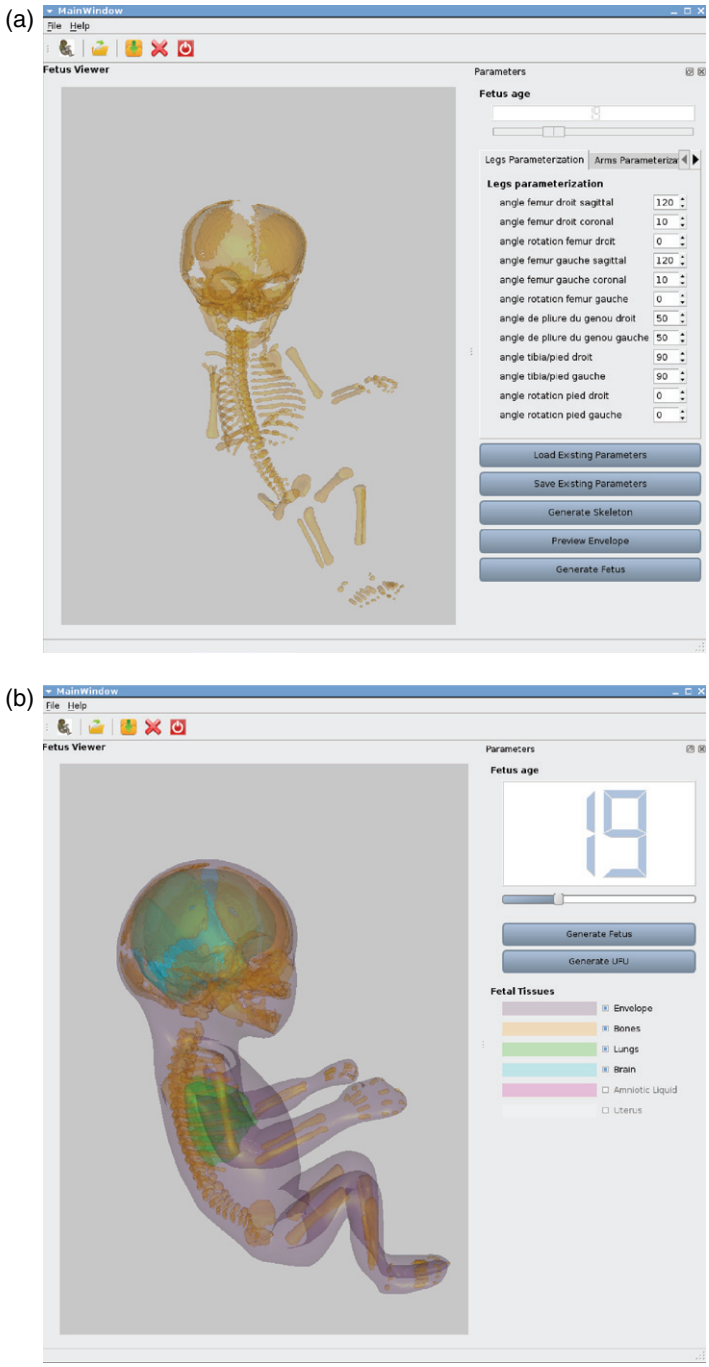

Figure 7. Illustrations of the fetal growth modeling tool user interface.

Illustrations of the software interface can be seen in figure 7.

Using this method, fetal models composed of the envelope, the skeleton, the brain and the lungs can be constructed and positioned in a realistic conformation as shown in figure 8.

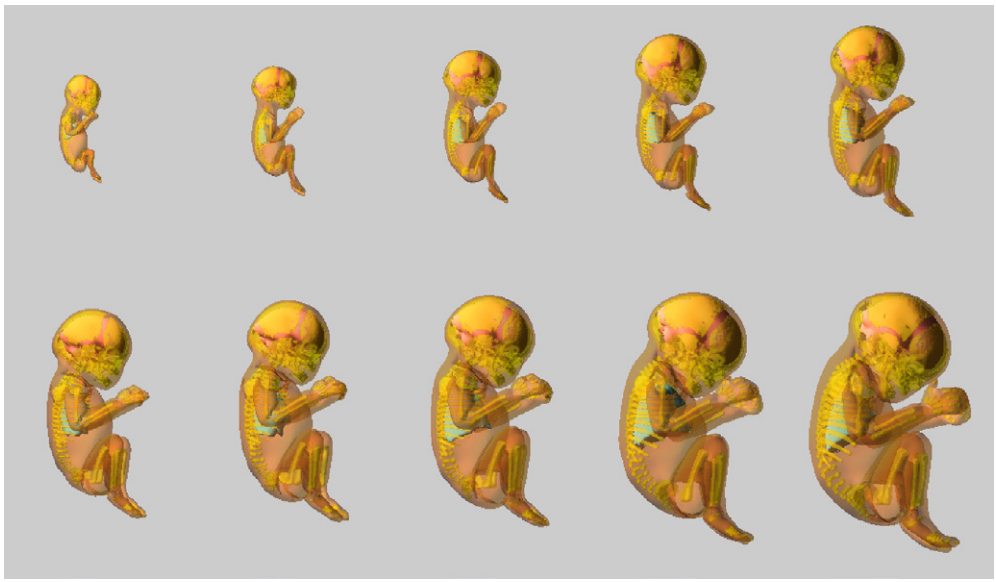

Figure 8. Generated fetuses using the proposed method. Fetuses ages are ranging from 14 to 32 WA with a two weeks step.

3.3. Utero fetal unit modeling

Once the embryo and fetuses modeling developed, one needs to reconstruct the whole Utero Fetal Unit (UFU) in order to be able to build a pregnant woman model. However, while in some cases, i.e. in 3D US data, we can manually segment the placenta and the amniotic liquid, these structures are difficult to generate automatically. Thus, two different strategies are proposed for the UFU reconstruction depending on the age of the fetus. For embryo models constructed directly from data segmentation, the whole UFU was segmented manually and reconstructed. For fetuses belonging to the second and third trimesters of pregnancy, a generic method based on medical charts (Uterus Charts) was developed. Indeed, since the shape of the UFU depends on the position of the mother and the fetus, no real study on this shape variability exists and only charts giving main diameters are available. To overcome this issue, we decided here to construct an egg-shaped uterus computed from the convex hull of the fetus envelope. The uterus and the amniotic liquid are then built around this convex hull while respecting the diameters given as reference by medical charts.

Since the UFU modeling is different for embryos and fetuses, and in order to assess the impact of this modeling on dosimetry results, the same generic modeling was also applied for first trimester embryos and thus both manual and automatic models are available for the earlier ages of pregnancy. Results of both manual and automatic modeling procedures are illustrated in figure 9. As we can see, while both manual and automatic volumes for the uterus are equivalent, their shapes vary greatly, which could be an issue for the dosimetry studies. Both options are thus proposed in the modeling tool.

4. Pregnant woman model construction

As detailed previously, high quality obstetric images have become readily available, allowing the construction of realistic models of the fetus at different stages of gestation. Unfortunately,

Figure 9. Comparison between an automatic generation (left figure) of the UFU and a manual segmentation (right figure) for a 13 WA old fetus. Fetal envelope (brown), amniotic fluid (yellow) and uterine wall (light brown) are displayed.

the field of view being usually focused on the fetus, the anatomy of the mother is only partially visible on the images and a full model of the pregnant woman can only be based on deformations of a non-pregnant woman body envelope (de la Plata Alcalde *et al* 2010).

While UFU modeling has been dealt with in the previous sections, the insertion of this unit and thus the construction of a pregnant woman model has yet to be addressed. This is done using the method presented in de la Plata Alcalde *et al* (2010).

As described in Bibin *et al* (2010) and de la Plata Alcalde *et al* (2010), (2011), the developed pregnant women models are composed of three components: (i) a set of previously constructed UFU (detailed in the previous section), (ii) an empty woman body envelope provided by Daz Studio (Daz 3D Studio), called Victoria, (iii) the pelvis bone and lumbar vertebrae of a pregnant woman, segmented on a CT data set of a subject having the same height as Victoria (167 cm), provided in Angel *et al* (2008). Insertion of the UFU relies on physics-based deformations using Simulated Open framework Architecture (SOFA) (Allard *et al* 2007) of the woman body to create realistic and flexible semi-homogeneous models of pregnant women. Victoria's body is positioned in standing position inside the simulated scene. A partial skeleton (pelvis bone and lumbar vertebrae) is placed inside Victoria's body interactively and three landmark points are manually selected on the skeleton: the two femoral head centers and the center of the vertebral disk between the L3 and L4 lumbar vertebra. The procedure to insert the UFU inside Victoria was introduced in Bibin *et al* (2010) and de la Plata Alcalde *et al* (2011) and is sumarized here.

The choice of these three points was made conjointly with a medical expert to insure accurate UFU positioning. These three points are clearly determined on medical images and a rigid transformation is performed to minimize the distance between the images and Victoria landmark points. After insertion, the UFU is scaled down, rotated by an angle of 20 degrees and then scaled up progressively. The progessive scaling ensures that the various maternal tissues are correctly deformed under the action of fetal growth. A final rotation is performed to reorient the fetus for Victoria in a standing position.

Since abdominal fat layers play an important role in dosimetry studies, an abdominal fat layer was also added to the pregnant woman model and an interactive tool allowing the control of the amount of fat added was developed using SOFA. A muscle layer was also modeled. This allows the simulation of pregnant-women models with identical morphology but different muscle and fat layer thicknesses.

The combination of the pregnant woman model construction and the UFU building described in the previous sections allows us to construct as many pregnant women models as

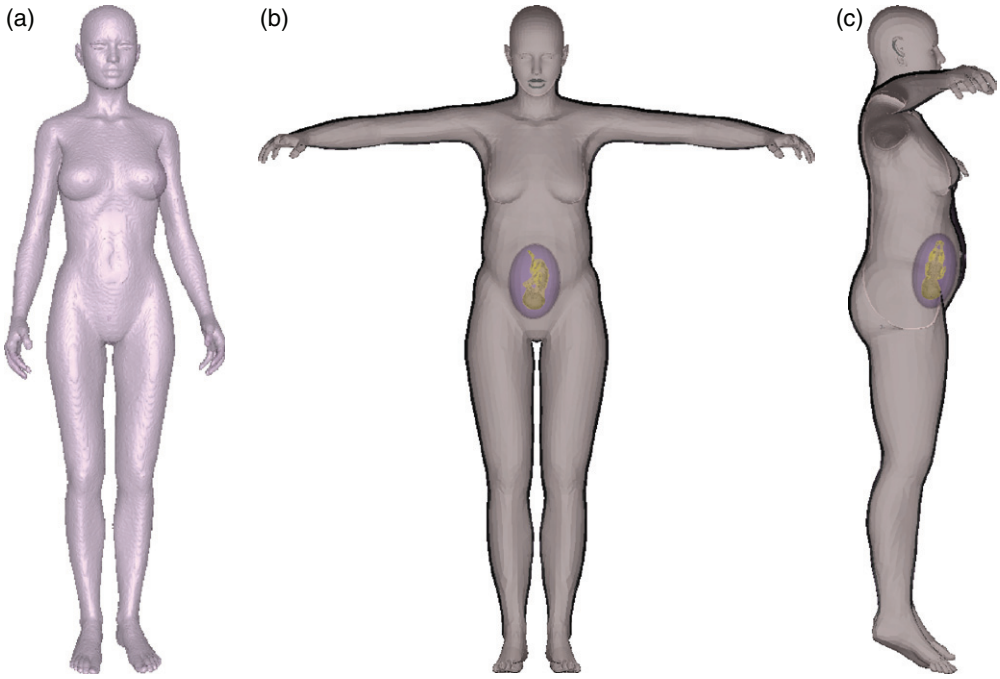

Figure 10. Initial and pregnant woman whole body model at 18 WA.

Table 2. Modeled structures available for two ranges of gestational ages (in WA).

Modeled structures	8–13 WA	14–32 WA
Fetal brain	X	X
Fetal lungs		X
Fetal skeleton		X
Fetal envelope	X	X
Uterus	X	X
Amniotic Liquid	X	X
Yolksac	X	
Umbilical cord	X	
Woman fat	X	X
Woman muscle	X	X
Woman envelope	X	X

we want between 8 and 32 WA. An example of such models can be seen in figure 10 where a pregnant woman with a fetus at 18 WA is displayed. Table 2 summarizes, for each stage of pregnancy, the available maternal and fetal tissues available.

5. Results

When dealing with image processing methods, object reconstruction and interpolation, one needs to be careful with the errors induced by the various data processing steps. Our method being built using mainly single samples for each gestational age, it is important to validate both the accuracy as well as the genericity by verifying that our generated models are close

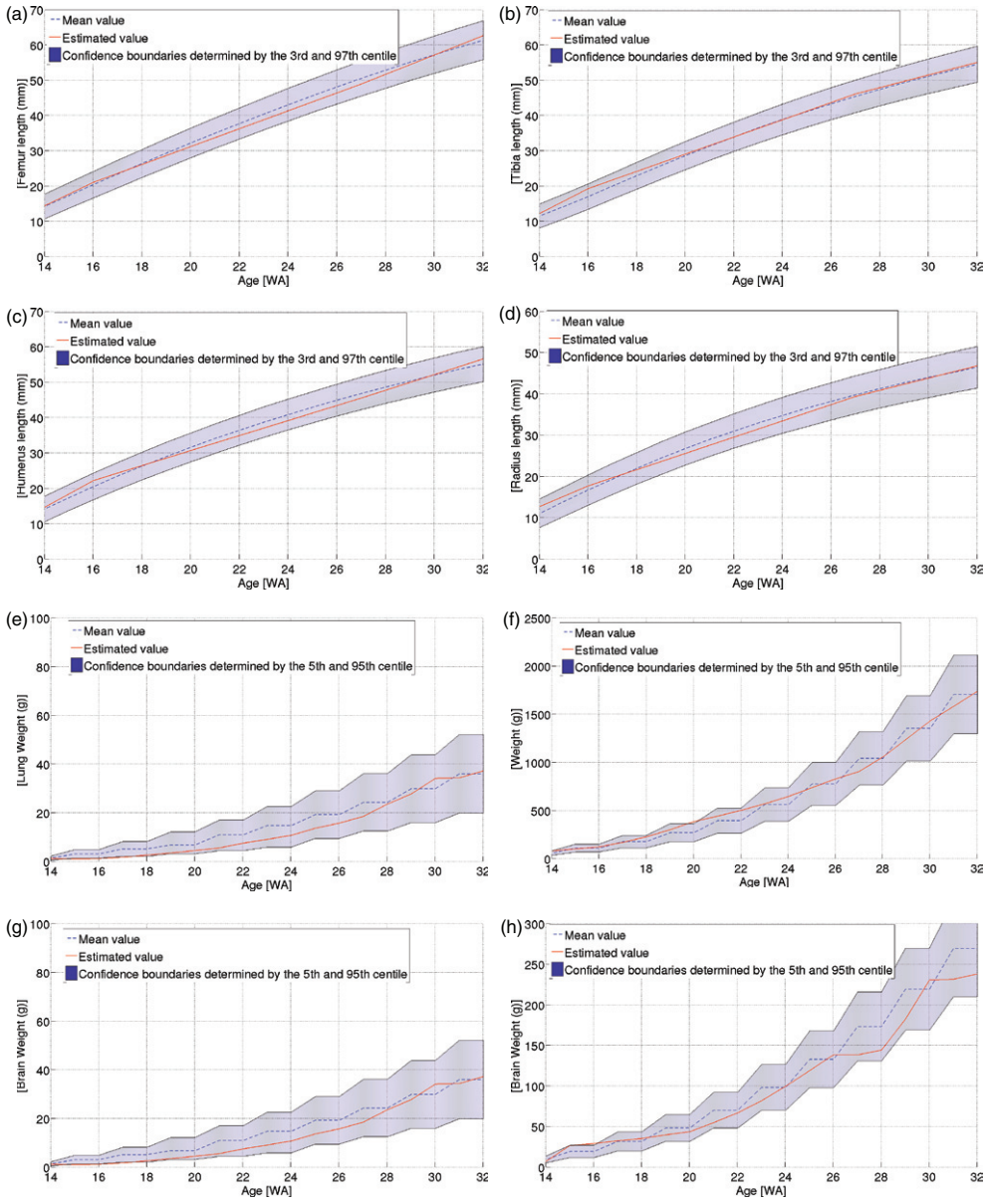

Figure 11. (*a*)–(*d*) Means of left and right values for the length of different fetus limbs (Femur, Tibia, Humerus, Radius) in relation to fetus ages (red) superimposed on charts values. In each case, the mean chart value as well as the confidence interval defined by the 3rd and 97th percentile are also drawn. These new simulations give similar results as the one obtained in our preliminary work in Serrurier *et al* (2013). (*e*) Bi-parietal diameter is also displayed using the same confidence intervals ranges. (*f*)–(*h*) Body, brain and lungs weights in relation to fetus ages (red) superimposed on charts values. In each case, the mean chart value as well as the confidence interval defined by the 5th and 95th percentiles are also drawn.

enough to a mean fetal model to be representative. Note that our aim is to build models representative enough but not statistical atlases.

5.1. Fetal model validation

In order to investigate both aspects, one fetal model per week is constructed from 14 to 32 WA. Standard biometric measures, classically used as growth biometrical markers, are computed on the generated models for all ages. They are completed by assessing the bone structure dimensions for the fetuses and compared to medical charts (Fetal Charts, Lyn and Douglas 2002). Figures 11 presents the obtained results for bi-parietal diameter, fetal weight, brain weight, lungs weight, femur, humerus, radius and tibia lengths and cranial perimeter. Weights were calculated using density estimates given in ICRP (1989) and Density Estimation, and reported in table 3.

Results, which complete the ones presented in Serrurier *et al* (2013), validate the proposed method. Indeed, biometrical values are always within the confidence intervals defined in the reference medical charts.

5.2. Fetal exposure to radiofrequency EMF: dosimetry results

In order to investigate the usability of our method for radiofrequency (RF) dosimetry studies, two different types of simulations were carried out.

The first one analyzes the variability of fetal exposure to EMFs with regard to the mother's morphology. Using the framework presented in the previous sections, two pregnant women models at 30 WA were constructed. For the first one, the abdominal fat layer was expanded to obtain an overweighted woman (OM) while for the second one, the abdominal fat layer was designed to obtain a pregnant woman with a normal corpulence (NM).

The dielectric properties of the adult's tissues were set using the values given in Gabriel *et al* (1996a), Gabriel (1996b), Gabriel (1996c)]. Following Hand *et al* (2006), the amniotic fluid was assumed to have the same dielectric properties as the cerebrospinal fluid. Finally, fetal tissues dielectric properties were set using the work of Peyman and Gabriel (2012), as summarized in table 4. According to Peyman and Gabriel (2012), there are no significant differences between dieletric properties of fetal tissues at different stages of pregnancy. Thus, a unique value is used here for each tissue, during the whole pregnancy.

A far-field exposure using an incident plane wave, polarized vertically, with a left side incidence and a frontal incidence, emitting at a frequency of 2100 MHz was simulated. To reduce computation time, both models were truncated to retrieve only the upper body. The total power absorbed by the fetus and the Specific Absorption Rate (SAR) distributions were evaluated using the well-known Finite Difference Time-Domain (FDTD) method (Taflove). The SAR, expressed in W kg^{-1}, quantifies the exposure to EMFs and represents the power absorbed per unit mass of tissue.

Figure 12 shows the SAR distributions induced in both pregnant woman models by the two different incident plane waves used.

We can remark here that depending on the woman's morphology and the type of waves used, fetal exposure seems to vary. To confirm this hypothesis, we computed for each configuration the total power absorbed by the fetus using an incident field $E = 1$ V m^{-1} (Surface Power Density $DSP = 2.65\ e^{-3}$ W m^{-2}). Results are reported in table 5.

According to these results, an hypothesis regarding the influence of the characteristics of incident waves used on fetal absorption can be made. Indeed, for both models, a frontal incidence plane wave leads to a higher absorption rate. Moreover, the women's corpulence

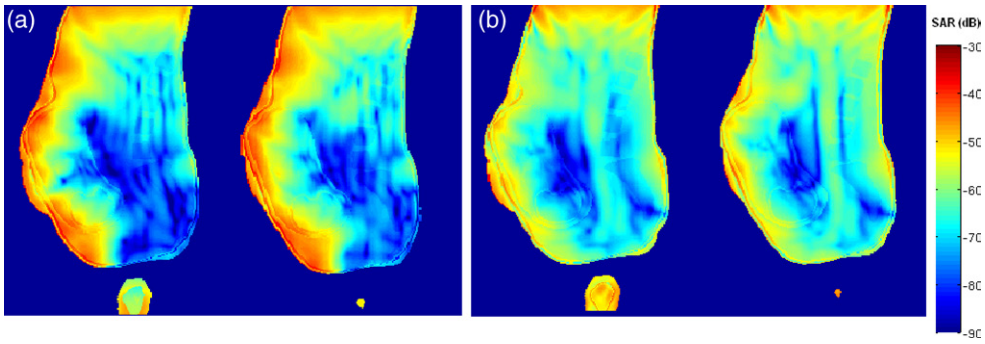

Figure 12. SAR distributions induced, in the maternal upper bodies of respectively the OM model and the NM model and their fetus, by the use of two different plane waves: (*a*) frontal incidence, (*b*) side incidence.

Table 3. Tissues densities used in this study.

Tissue	Density value (kg m^{-3})
Fetal brain	1020
Fetal lungs	722
Fetal skeleton	1650
Fetal soft tissues	1050
Uterus	1026
Uterus content	1007
Woman fat	916
Woman muscle	1047
Woman homogeneous tissues	1048
Woman skin	1125
Woman pelvis	1850

Table 4. Dielectric properties used in this work.

Tissue	Permitivity F m^{-1}	Conductivity S m^{-1}
Fetal brain	62.5	1.88
Fetal lungs	34.80	1.08
Fetal skeleton	37	1.28
Fetal soft tissues	59.3	1.89
Uterus	58.4	1.97
Uterus content	68.42	2.22
Woman fat	5.31	0.08
Woman muscle	54.03	1.57
Woman homogeneous tissues	14.64	0.45
Woman skin	40.89	1.34
Woman pelvis	15.276	0.50

seems to play an important role in fetal protection with regard to electromagnetic waves. While it is difficult to draw definite conclusions based only on two simulations, a hypothesis concerning the impact of the pregnant woman abdominal fat layer on the fetal exposure can be formulated, the thicker the abdominal fat layer, the lower the fetal exposure would be.

The second one, analyzes the influence of the pregnancy stage on the fetus exposure to radiofrequency EMF using an incident plane wave polarized vertically, with a frontal incidence,

Table 5. Total power absorbed by the fetus for each pregnant woman model and each plane wave configuration.

Plane wave incidence	Total power absorbed by the fetus inside OM (in W)	Total power absorbed by the fetus inside NM (in W)	Difference (in % of the total power absorbed in OM)
Frontal	4.66e-6	5.38e-6	+ 15.48
Side	8.36e-7	1.06e-6	+ 26.58

emitting at the frequency of 2100 MHz. SAR distribution results are shown in figure 13 where fetal exposure to plane waves at different stages of pregnancy is studied.

Preliminary results comparing the exposure with a complete model and with a truncated one show that truncating the maternal body leads to an overestimation of fetal whole body and brain exposure. However, the values remain below the recommended limits in both cases, and relative values (for instance between models with different fat thicknesses, or at different ages) are not affected by the fact that the model is truncated. Moreover, the use of truncated models allows us to take the details in the abdominal tissues into account, while reducing the computation time.

The results presented above illustrate the usefulness of the fetus and pregnant woman model presented in this paper in numerical dosimetry studies. Indeed, the possibility to generate different fetuses at different ages, in different positions and in different conformations (head up or down) as well as different types of pregnant women allows us to investigate a large field of dosimetry related questions.

6. Conclusion and discussion

In this paper, a fetal growth modeling tool allowing the construction of numerical models of the fetal body at any gestational age and position between 8 and 32 WA has been proposed. This tool relies on data acquired almost entirely during *in vivo* medical exams of pregnant women. A growth simulation method, combined with a method to insert the fetus into a woman body, allowed us to propose a highly configurable tool for the construction of a wide variety of fetus models at different ages and in different positions inserted in different women morphologies. This process ensures realistic models but raises also few concerns due to the heavy processing involved with medical images. The model relies indeed on a limited number of subjects not allowing us to take into account the variability between fetuses of a same age. This may induce a bias in the evolution model since inter-individual variability cannot be stretched apart from inter-ages variability. The validity of the models regarding fetal age and position has been studied via comparisons with chart values. Despite the modest size of the initial database, this validation has shown that the modeled fetuses are of high quality in terms of biometry measures and visual appearance. Increasing the size of the image database will naturally improve the precision and allow even more realistic models by including more internal organs for example. The tool proposed here covers most part of the fetal gestation and can be easily used in a wide variety of dosimetry studies as illustrated by the numerical dosimetry experiments carried out in this paper. Finally, despite all the aforementioned limitations, this model represents, as far as we know, one of the first models combining the growth of the fetus (including skeleton, envelope, brain and lungs), an original skeleton-driven repositioning and a pregnant woman modeling using physical constraints. This allows the estimation of a fetus at any age and position and its insertion in a woman model with various sizes of abdominal fat layers.

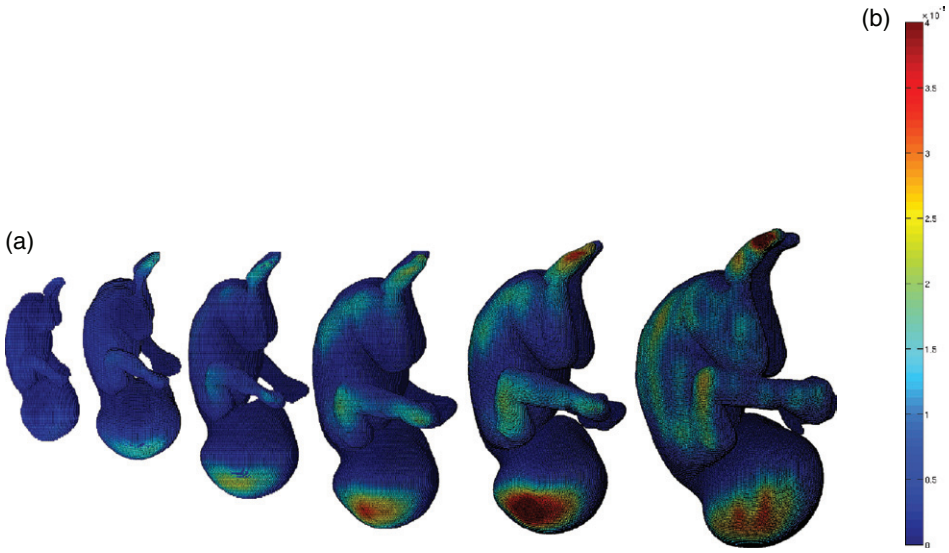

Figure 13. SAR distributions induced inside the fetal body.

Acknowledgments

The authors would like to thank the hospitals of St Vincent de Paul and Kremlin Bicetre (Professor C. Adamsbaum, Dr V Calmels), Port-Royal (Professor G Grangé) and Beaujon (Professor D Luton) for providing medical data expertise. They would also like to thank Professor G Captier at the Anatomy Laboratory in Montpellier for the fetal specimens, and Dr T Nagaoka from the National Institute of Information and Communications Technology of Tokyo for the 3D mesh at 20 WA. Finally, they would like to thank Daz 3-D Studio for providing the Victoria model. This work has been funded by the ANR-JST FETUS project.

Some of the fetus models are available at http://femonum.femonum.telecom-paristech.fr/.

References

Allard J, Cotin S, Faure F, Bensoussan P-J, Poyer F, Duriez C, Delingette H and Grisoni L 2007 SOFA: an open source framework for medical simulation *MMVR 15: Medicine Meets Virtual Reality (Studies in Health Technology, Informatics* vol 125) (Amsterdam: IOP) pp 13–8

Angel E *et al* 2008 Radiation dose to the fetus for pregnant patients undergoing multidetector CT imaging: Monte Carlo simulations estimating fetal dose for a range of gestational age and patient size *Radiology* **249** 220–7

Anquez J, Angelini E D and Bloch I 2009 Automatic Segmentation of Head Structures on Fetal MRI *IEEE Int. Symp. on Biomedical Imaging (ISBI) (Boston, Jun. 2009)* pp 109–12

Anquez J, Angelini E D, Bloch I, Merzoug V, Bellaiche-Millischer A E and Adamsbaum C 2007 Interest of the Steady State Free Precession (SSFP) sequence for 3D modeling of the whole fetus *Engineering in Medicine and Biology Conf. EMBC 2007 (Lyon, Aug. 2007)* pp 771–4

Anquez J, Angelini E D, Grangé G and Bloch I 2013 Automatic segmentation of ante-natal 3D ultrasound images *IEEE Trans. Biomed. Eng.* **60** 1388–400

Becker J, Zankl M, Fill U and Hoeschen C 2008 Katja, the 24th week of virtual pregnancy for dosimetric calculations *Polish J. Med. Phys. Eng.* **14** 13–20

Bibin L, Anquez J, de la Plata Alcalde J P, Boubekeur T, Angelini E D and Bloch I 2010 Whole-body pregnant woman modeling by digital geometry processing with detailed uterofetal unit based on medical images *IEEE Trans. Biomed. Eng.* **57** 2346–58

Bibin L, Anquez J, Hadjem A, Angelini E D, Wiart J and Bloch I 2009 Dosimetry studies on a fetus model combining medical image information, synthetic woman body *11th World Congress on Medical Physics, Biomedical Engineering (Munich, Sept. 2009)* pp 321–4

Chen J 2004 Mathematical models of the embryo and fetus for use in radiological protection *Health Phys.* **86** 285–95

Cristy M and Eckerman K F 1987 Specific absorbed fractions of energy at various ages from internal photon sources *Technical Report* (Oak Ridge National Laboratory)

Dahdouh S, Serrurier A, Grangé G, Angelini E D and Bloch I 2013 Segmentation of fetal envelope from 3D ultrasound images based on pixel intensity statistical distribution, shape priors *Int. Symp. Biomedical Imaging: From Nano to Macro ISBI'13 (San Francisco, Apr. 2013)* pp 1014–7

Daz 3D Studio www.daz3d.com/

de la Plata Alcalde J P, Bibin L, Anquez J, Boubekeur T, Angelini E D and Bloch I 2010 *Physics-based modeling of the pregnant woman ISBMS (Phoenix, Jan. 2011)* (Berlin: Springer) pp 71–81

de la Plata Alcalde J P, Anquez J, Bibin L, Boubekeur T, Angelini E D and Bloch I 2011 FEMONUM: a framework for whole body pregnant woman modeling from ante-natal imaging data *Proc. of the Eurographics 2011 Medical Prize Awards* (Liandudno, Wales)

Density Estimation www.itis.ethz.ch/itis-for-health/tissue-properties/database/density

Dimbylow P 2006 Development of pregnant female, hybrid voxel-mathematical models and their application to the dosimetry of applied magnetic and electric fields at 50 Hz *Phys. Med. Biol.* **51** 2383

Fetal charts from the French College of Fetal Ultrasonography www.cfef.org/archives/communication/biometrie2000/selectframe.html

Gabriel C, Gabriel S and Corthout E 1996a The dielectric properties of biological tissues: I. Literature survey *Phys. Med. Biol.* **41** 2231

Gabriel S, Lau R W and Gabriel C 1996b The dielectric properties of biological tissues: II. Measurements in the frequency range 10 Hz to 20 GHz *Phys. Med. Biol.* **41** 2251

Gabriel S, Lau R W and Gabriel C 1996c The dielectric properties of biological tissues: III. Parametric models for the dielectric spectrum of tissues *Phys. Med. Biol.* **41** 2271

Guihard-Costa A-M and Larroche A-M 1995 Fetal biometry, growth charts for practical use in fetopathology and antenatal ultrasonography *Fetal Diagn. Ther.* **10** 212–79

Hand J W, Li Y, Thomas E L, Rutherford M A and Hajnal J V 2006 Prediction of specific absorption rate in mother and fetus associated with MRI examinations during pregnancy *Magn. Reson. Med.* **55** 883–93

Hadjem A, Conil E, Bibin L, Anquez J, Angelini E D, Bloch I and Wiart J 2010 Analysis of the SAR induced in the fetus at different stages of gestation exposed to plane wave at 900 MHz *Annual Meeting of The Bioelectromagnetics Societyg (BEMS) (Seoul, Jun. 2011)*

ICRP 1989 ICRP publication 89: basic anatomical and physiological data for use in radiological protection: reference values *Technical Report*

ICRP 2003 ICRP publication 90: biological effects after prenatal irradiation (embryo and fetus) *Technical Report*

Lyn S C and Douglas G A 2002 Charts of fetal size: limb bones *BJOG: Int. J. Obstet. Gynaecol.* **109** 919–29

Maynard M R, Geyer J W, Aris J P, Shifrin R Y and Bolch W 2011 The UF family of hybrid phantoms of the developing human fetus for computational radiation dosimetry *Phys. Med. Biol.* **56** 4839

Nagaoka T, Saito K, Takahashi M, Ito K and Watanabe S 2008 Anatomically realistic reference models of pregnant women for gestation ages of 13, 18 and 26 weeks *Conf. Proc. IEEE Eng. Med. Biol. Soc.* **2008** 2817–20

Peyman A and Gabriel C 2012 Dielectric properties of rat embryo and foetus as a function of gestation *Phys. Med. Biol.* **57** 2103

Serrurier A, Dahdouh S, Captier G, Calmels V, Adamsbaum C and Bloch I 2013 3D articulated growth model of the fetus skeleton, envelope, soft tissues *Innov. Res. Biomed. Eng.* **34** 349–56

Shi C and Xu X G 2004 Development of a 30 week-pregnant female tomographic model from computed tomography (ct) images for monte carlo organ dose calculations *Med. Phys.* **31** 2491–7

Stabin M G, Watson E, Cristy M, Ryman J C, Eckerman K F, Davis J, Marshall D and Gehlen K 1995 Mathematical models, specific absorbed fractions of photon energy in the nonpregnant adult female and at the end of each trimester of pregnancy *Technical Report* (Oak Ridge National Laboratory)

Taflove A and Hagness S C 2005 A Computational Electrodynamics: the Finite-Difference Time-Domain Method 2nd edn (Boston, MA: Artech House)

Uterus Charts www.aly-abbara.com/echographie/biometrie/hauteur_uterine.html

Vese L A and Chan T F 2002 A multiphase level set framework for image segmentation using the Mumford-Shah model *Int. J. Comput. Vis.* **50** 271–93

Wiart J, Watanabe S, Bloch I, Anquez J, de la Plata Alcalde J P, Angelini E D, Boubekeur T and Faraj N 2011 Exposure to fetus to RF. preliminary results assessed with different realistic 3D numerical models *33rd Annual Meeting of the Bioelectromagnetics Society (Halifax, Jun. 2011)* (Frederick: Bioelectromagnetics Society)

Xu X G, Chao T C and Bozkurt A 2000 Vip-man: an image-based whole-body adult male model constructed from color photographs of the visible man project for multi-particle Monte Carlo calculations *Health Phys.* **78** 476–86

Xu X G, Taranenko V, Zhang J and Shi C 2007 A boundary-representation method for designing whole-body radiation dosimetry models: pregnant females at the ends of three gestational periods–RPI-P3, -P6 and -P9 *Phys. Med. Biol.* **52** 7023–44

Zhu Y and Gortler S J 2007 3D deformation using moving least squares *Technical Report* Harvard University, Cambridge